STUDIA UBB CHEMIA, LXX, 4, 2025 (p. 41-55)
(RECOMMENDED CITATION)
DOI:10.24193/subbchem.2025.4.03

STUDY OF ELECTROCHEMICAL BEHAVIOR OF VI-B GROUP METAL OXIDES IN TUNGSTATE MELT

Victor MALYSHEV[a], Angelina GAB[a], Ana-Maria POPESCU[b]*, Virgil CONSTANTIN[b]*

ABSTRACT. Thermodynamic assessment of the probability of interaction of metal oxides of group VI-B with tungstate melts, the results of the study of the acid-base properties of tungstate melt by potentiometric method. Analysis of the presented experimental data on the study of the electrochemical behavior of chromium, molybdenum and tungsten under equilibrium and non-equilibrium conditions allows us to conclude that it is possible to implement multi-electron reversible equilibria and electroreduction processes involving oxide forms of chromium, molybdenum and tungsten (VI) in tungstate melts. The mechanism and final product of electroreduction of oxide forms of metal (VI) depend on the acid-base properties of the medium. By setting the latter, it is possible to control the electrode process.

Keywords: *VI-B group metals, thermodynamic assessment, electrochemical behavior, multielectron processes.*

INTRODUCTION

Melts based on tungstates of alkali and alkaline-earth metals are practically important for the production of VI-B group metals in the form of dispersed powders [1-5] and coatings [1, 4, 6-9], of alloys and intermetallics [9-11], of oxides and bronzes of various stoichiometric compositions [1, 12, 13], as well as for the synthesis of compounds with nonmetals (carbides, borides, silicides, phosphides, sulfides) [13-16]. The composition of cathode precipitates

[a] *International European University, 42 V Academician Glushkov Avenue, 03187, Kyiv, Ukraine*
[b] *Romanian Academy, "Ilie Murgulescu" Institute of Physical Chemistry, Laboratory of Electrochemistry and Corrosion, 202 Splaiul Independentei, 060021, Bucharest, Romania*
* *Corresponding authors: virgilconstantin@yahoo.com, popescuamj@yahoo.com*

in these melts is largely determined by the acid-base properties of the melts [17-20]. As compounds influencing the acidity basicity) of tungstate melts, particularly VI-B group metal oxides can be used, which can act not only as acceptors of oxygen ions, but also as components in the electrochemical production of metals and in the synthesis of their compounds.

Statement of the problem. The aim of the work is to study the electrochemical behavior of VI-B group metal oxides in tungstate melts and to identify the possibility of the existence of equilibria involving VI-B group metal electrodes. Achieving this goal will make it possible to control the acid-base properties of melts and to use the results of studies of the electrochemical behavior of VI-B metal oxides in tungstate melts for the practical implementation of electrodeposition of VI-B metals and their compounds.

RESULTS AND DISCUSSION

1. Thermodynamic assessment of the probability of interaction of group VI-B metal oxides with tungstate melts. The literature contains virtually no information on the chemical interactions of tungstate melts with group VI-B metal oxides. We performed thermodynamic calculations of possible reactions of interaction of these oxides with sodium tungstate (Table 1). It can be seen that chromium (VI), molybdenum (VI), and tungsten (VI) oxides are likely to interact with these melts to form dimeric compounds. Although the performed thermodynamic calculations suggest only the possibility of reactions for tungstate melts, they can be quite useful in explaining the model of the ionic composition of the melt. According to the calculations, the most energetically beneficial reactions are those involving the formation of ditungstate compounds.

Table 1. Temperature dependence of the standard free energy ΔG^o_T of the interactions of sodium tungstate with oxygen-containing group VI-B elements compounds.

Nr.	Reactions	ΔG^o_T, kJ				
		298 K	900 K	1000 K	1100 K	1200 K
1.	$2Na_2WO_4 + 2CrO_3 = Na_2Cr_2O_7 + Na_2W_2O_7$	-131.37	-409.81	-365.01	-320.62	-284.88
2.	$2Na_2WO_4 + CrO_3 = Na_2CrO_4 + Na_2W_2O_7$	-79.73	-234.25	-211.19	-109.51	-165.81
3.	$Na_2WO_4 + MoO_3 = Na_2MoO_4 + Na_2W_2O_7$	-44.35	-53.51	-47.49	-43.60	-37.74
4.	$2Na_2WO_4 + 2MoO_3 = Na_2Mo_2O_7 + Na_2W_2O_7$	-79.91	-94.77	-83.68	-70.12	-57.32
5.	$Na_2WO_4 + WO_3 = Na_2W_2O_7$	-23.26	-32.30	-27.03	-23.93	-22.68

2. Study of tungstate melt acid-base properties by methods of potentiometry of cooled samples. To explain the experimental dependences of the tungstate melts behavior under equilibrium and nonequilibrium conditions, the following model of the ionic composition of such melts can be proposed, considering oxygen-containing compounds as conjugated acids-bases. It is assumed that in the Na_2WO_4 melt, the ions Na^+, $(WO_4)^{2-}$, $(W_2O_7)^{2-}$, and $(O)^{2-}$ are predominantly present, which are in equilibrium with each other. So, this can be considered as molten polytungstate electrolyte of the composition $2Na^+ + (W_nO_{2n+1})^{2-}$, where $n > 1$. The shift in interionic equilibria in such melt can be explained by a "quasi-chemical" approach. When chromium, molybdenum, and tungsten oxides are added to the tungstate melt, the following reactions are possible (Table 1): for CrO_3 - (1) and (2), MoO_3 - (3) and (4), WO_3 - (5). To study changes in the oxygen ions activity in such melts, electrochemical cells with oxygen electrodes can be used:

$$(-)Pt|O_2|(1 - n)\ Na_2WO_4\text{-}MO_3|\beta\text{-}Al_2O_3|0.8\ Na_2WO_4\text{-}0.2\ WO_3|O_2|Pt(+), \quad (1)$$

where M = Cr, Mo, or W. In this case, one of the electrodes is semi-immersed into a stable-composition melt with known oxygen ions activity. The study was carried out in air at a constant oxygen partial pressure above the melt ($P(O_2)$ = 21.3 kPa). The diffusion potential value between the studied melt and the reference electrode melt was negligible and, according to calculations, did not exceed $3 \cdot 10^{-3}$ V (since alkali metal cations play a major role in the current transfer process [21, 22]. Therefore, the oxygen electrode potential is practically determined by the ratio of the oxygen ions activities in the studied melt and in the reference electrode melt. At low concentrations of oxygen ion acceptors, the tungstate melt consists mainly of Na+, $(WO_4)^{2-}$, $(W_2O_7)^{2-}$, and $(O)^{2-}$ ions. At a high acceptors concentration, it is also necessary to take into account the presence of $(W_3O_{10})^{2-}$, $(W_4O_{13})^{2-}$, and other more complex particles.

From the dependence of the equilibrium potential of the oxygen electrode on the concentrations of group VI-B metal oxides (Fig. 1), it follows that its value shifts to the positive region when the oxides are introduced into the tungstate melt. Thus, these oxides are oxygen ions acceptors. Such a course of dependencies can be explained by considering oxygen-containing compounds as conjugated acids-bases. There is an equilibrium in the tungstate melt:

$$2\ (WO_4)^{2-} \leftrightarrow (W_2O_7)^{2-} + (O)^{2-} \quad (2)$$

with an equilibrium constant (K):

$$K = \frac{\left[WO_4^{2-}\right]^2}{\left[W_2O_7^{2-}\right]\left[O^{2-}\right]} \quad (3)$$

When CrO_3, MoO_3, or WO_3 oxides are added to the sodium tungstate melt, dichromate, dimolybdate, and ditungstate ions can also be formed according to reactions (1), (4), and (5), respectively.

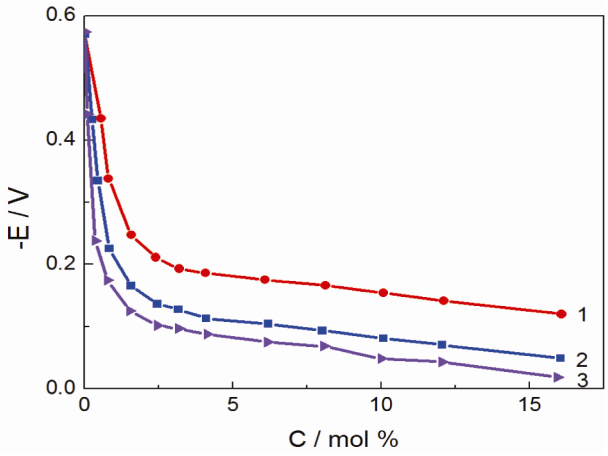

Figure 1. Equilibrium potentials of the oxygen electrode when metal oxides of group VI-B are introduced into the sodium tungstate melt: 1 - Cr_2O_3; 2 - MoO_3; 3 - WO_3; T = 1173 K.

3. Electroreduction of chromium (VI), molybdenum (VI) and tungsten (VI) oxides on the background of tungstate melt. In the stationary and non-stationary voltammetric dependences (Figs. 2a and 2b) of the tungstate melt containing group VI-B metal oxides with an oxidation degree of metal equal to +6, a reduction wave was observed at potentials from -0.7 V to -1.0 V for CrO_3, from -0.9 V to -1.2 V for MoO_3, and from -1.1 V to -1.3 V for WO_3. At concentrations of MoO_3 and WO_3 of around $(3\div6)\times10^{-4}$ mol/cm^3, the main wave is preceded by an alloying wave. The possibility of the existence of intermetallics is confirmed by data [23]. At higher oxides concentrations, the alloying wave disappears, because the potential of the main process becomes more positive. In the case of addition of CrO_3 to the tungstate melt, the alloying wave is not observed, since in this case the electroreduction product is chromium (III) oxide rather than chromium metal. An increase in the concentration of all three oxides leads to an increase in the wave height and its shift to the positive potentials region. In this case, the transformation of the extended wave into a sickle-like one is observed. The reduction process occurs in one stage. Increasing the scan rate up to 10 V/s does not allow one to detect the process stages sequence.

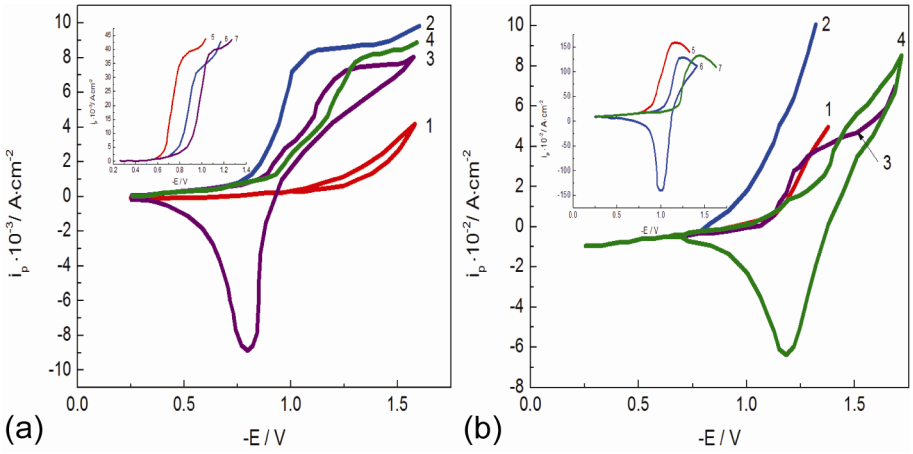

Figure 2. Stationary voltammetric dependences of the melt containing
a) MO_3 (M: Cr, Mo, W); 1 - Na_2WO_4 background; 2, 5 - CrO_3 addition [CrO_3]: $4\cdot10^{-4}$ mol/cm^3, $9\cdot10^{-4}$ mol/cm^3; 3, 6 - MoO_3 addition [MoO_3]: $4\cdot10^{-4}$ mol/cm^3, $9\cdot10^{-4}$ mol/cm^3; (4, 7) - WO_3 addition, [WO_3]: $4\cdot10^{-4}$ mol/cm^3, $9\cdot10^{-4}$ mol/cm^3; T = 1173 K, working electrode - platinum, scan rate - 0.02 V/s;
b) Na_2WO_4 melt; 1 - Na_2WO_4 background; 2, 5 - CrO_3 addition; [CrO_3]: $6\cdot10^{-4}$ mol/cm^3, $1\cdot10^{-3}$ mol/cm^3; 3, 6 - MoO_3 addition [MoO_3]: $6\cdot10^{-4}$ mol/cm^3, $1\cdot10^{-3}$ mol/cm^3; 4, 7 - WO_3 addition, [WO_3]: $6\cdot10^{-4}$ mol/cm^3, $1\cdot10^{-3}$ mol/cm^3; T = 1173 K, cathode - platinum, scan rate - 1.0 V/s.

Potentiostatic electrolysis at the observed wave potentials reveals the following products: in the case of CrO_3 - Cr_2O_3 oxide powder within the entire studied concentration range. This is confirmed by further calculations of the number of electrons for electrochemical processes that occur at platinum and chromium electrodes. In the case of WO_3 - metallic tungsten up to WO_3 concentrations 20 mol %, and in the case of MoO_3 - metallic molybdenum up to MoO_3 concentrations 4 mol %. If the concentration limits are exceeded, the electrolysis products are tungsten and molybdenum dioxides, respectively.

The peak current dependences on the oxide concentration at different scan rates are characterized by a directly proportional current increase with the oxide concentration change (Fig. 3). The ratio $i_p/v^{1/2}$ values from dependences of $i_p/v^{1/2}$ on $v^{1/2}$ remain practically constant within a wide range of scan rates from 0.04 up to 2.00 V/s (Fig. 4). The mass transfer constants i_p/nFc for stationary waves (calculated within the range of MO_3 (M = Mo, W) concentrations $(5\div15)\times10^{-4}$ mol/cm^3) are $(0.73\div2.23)\times10^{-4}$ cm/s and are commensurate with those for diffusion delivery. The direct proportional dependence of the limiting current on the metal (VI) oxide concentration, the constancy of the $i_p/v^{1/2}$ ratio values within a wide scan rates range, as well as

the i_p/nFc ratio value, indicate that the electrode process is limited by the diffusion of electroactive particles to the electrode surface. So, under these polarization regimes, the electroactive particles formation rate does not impose restrictions on the electrode process.

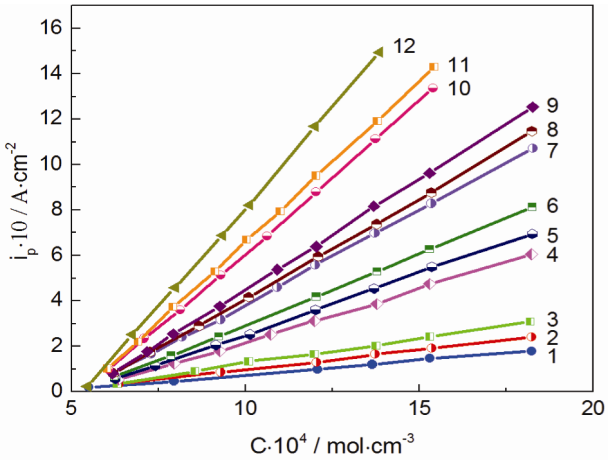

Figure 3. Peak current density dependence on the concentration of MO_3 (M = Mo, W) at different scan rates. 1 - MoO_3, 0.02 V/s; 2 - WO_3, 0.02 V/s; 3 - Cr_2O_3, 0.02 V/s; 4 - MoO_3, 0.50 V/s; 5 - WO_3, 0.50 V/s; 6 - Cr_2O_3, 0.50 V/s; 7 - MoO_3, 1.00 V/s; 8 - WO_3, 1.00 V/s; 9 - Cr_2O_3, 1.00 V/s; 10 - MoO_3, 5.00 V/s; 11 - WO_3, 5.00 V/s; 12 - Cr_2O_3, 5.00 V/s; T = 1173 K.

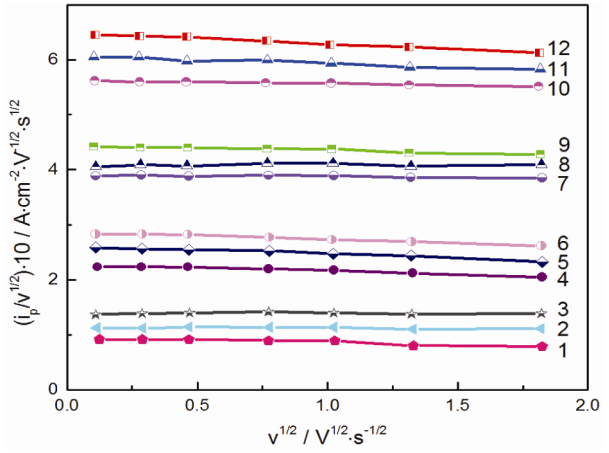

Figure 4. Dependence of $i_p/v^{1/2}$ on $v^{1/2}$ for the electroreduction process of chromium, molybdenum, and tungsten containing ions at $[MO_3]\times 10^4$, mol/cm^3: (1-3) - 7.0; (4-6) - 8.0; (7-9) - 10.0; (10-12) - 12.0; (1, 4, 7, 10) - MoO_3; (2, 5, 8, 11) - WO_3; (3, 6, 9, 12) - CrO_3. T = 1173 K, cathode - platinum, scan rate - 1.0 V/s

The mechanism of electroactive particles formation becomes clear if we proceed from the concept of the existence of acid-base equilibria in tungstate melts. The decrease in the activity of oxygen ions when MO_3 is added to the tungstate melt is evident in the dependences of the equilibrium potentials of the oxygen electrode (Fig. 1). The addition of MO_3 shifts this electrode potential toward positive values, i.e., reduces the oxygen ions activity in the melt. The sodium tungstate melt is quite stable and can be used as a background solvent for the electroreduction of chromium (molybdenum, tungsten) (VI) oxide forms. The first additions of MO_3 lead to the formation of predominantly monomeric $(MO_4)^{2-}$ ions; the concentration of dimeric $(M_2O_7)^{2-}$ ions is negligible. Monomeric forms exhibit electrochemical activity at potentials comparable to the background electrolyte decomposition potential. The further MO^3 addition leads to an increase in the concentration of dimeric $(M_2O_7)^{2-}$ ions which exhibit electrochemical activity at much more positive potentials.

These ideas are also confirmed by our thermodynamic calculations of possible reactions of MO_3 oxides with sodium tungstate (sodium molybdate). In the case of metal deposition, the electrode process can be summarized as follows:

$$(M_2O_7)^{2-} + 6e^- \leftrightarrow M + (MO_4)^{2-} + 3(O)^{2-};$$

or, taking into account the subsequent rapid chemical ionic reaction,

$$(O)^{2-} + (M_2O_7)^{2-} \leftrightarrow (2MO_4)^{2-};$$

the gross equation of the electrode process will be as follows:

$$4(M_2O_7)^{2-} + 6e^- \leftrightarrow M + 7(MO_4)^{2-}. \quad (4)$$

In the case of metal (IV) oxide deposition, these equations can be written as follows:

$$(M_2O_7)^{2-} + 2e^- \leftrightarrow MO_2 + (MO_4)^{2-} + (O)^{2-},$$

$$(O)^{2-} + (M_2O_7)^{2-} \leftrightarrow 2(MO_4)^{2-},$$

$$2(M_2O_7)^{2-} + 2e^- \leftrightarrow MO_2 + 3(MO_4)^{2-}. \quad (5)$$

In the case of metal (III) oxide deposition, these equations take the following form:

$$(M_2O_7)^{2-} + 6e^- \leftrightarrow M_2O_3 + 4(O)^{2-},$$

$$(O)^{2-} + (M_2O_7)^{2-} \leftrightarrow 2(MO_4)^{2-},$$

$$5(M_2O_7)^{2-} + 6e^- \leftrightarrow M_2O_3 + 8(MO_4)^{2-}. \quad (6)$$

To clarify the nature of the charge transfer stage (4)-(6), and to determine the number of electrons transferred in the electrode process, the stationary voltammetric dependences obtained at platinum electrodes were analyzed in the semilogarithmic coordinate system E-lg(i_d-i). The sickle-like shape of the stationary waves necessitates the use of the Kolthoff-Lingane equation. The composition of electrolysis products was studied by measuring the concentration in mol%. The slope of the E-lg(i_d-i) dependences for different CrO_3 concentrations is 39-42 mV, and the value of n = 5.8-6.1 (Fig. 5a). The theoretical value of the slope for the six-electron reversible reaction is 39 mV.

The slopes of E-lg(i_d-i) dependences for MoO_3 concentrations up to 4 mol % are 37-44 mV, and the values of n = 5.3-6.2. At the concentration of MoO_3 above 4 mol %, the slope of this dependence is 105-128 mV, and the value of n = 1.8-2.1 (Fig. 5b).

A polarization rate of 2 mV·s^{-1} corresponds to steady-state conditions. At such values, it is advisable to use the Kolthoff-Lingane equation (Table 2).

Table 2. The number of electrons transported in the electrode process of MoO_3 electroreduction in the Na_2WO_4 melt.

C(MoO_3)·10^4, mol·cm^{-3}	ΔE/lg(i_d-i)	n
1.0	0.038	6.1
2.0	0.039	5.9
4.0	0.042	5.5
6.0	0.105	2.2
8.0	0.117	2.0
9.0	0.112	2.1
11.0	0.120	1.9
13.0	0.125	1.9

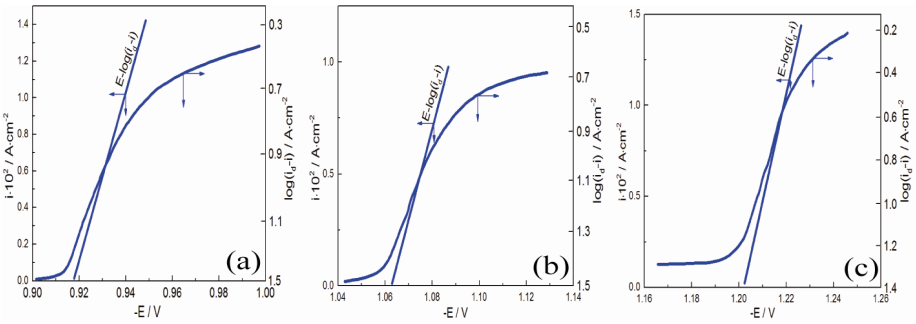

Figure 5. Analysis of steady-state voltammetric dependences in the semilogarithmic coordinate system. Scan rate - 2 mV/s; T = 1173 K; cathode - platinum; a) [CrO_3] = 2.5 mol %; b) [MoO_3] = 3 mol %; c) [WO_3] = 2.5 mol %.

The theoretical slope value for the two-electron reversible reaction is 112 mV. The slope of the E-lg(i_d-i) dependences for different concentrations of WO_3 is 38-45 mV, and the value of n = 5.5-6.2 (Fig. 5c). The coincidence of the slopes determined from the experimental data with the theoretical ones indicates the reversible nature of the charge transfer stages (4)-(6).

The reversible nature of the charge transfer stages also follows from the experimental results obtained.

The deposition potential and the half-wave potential do not depend on the scan rate up to 0.2-0.5 V/s (Fig. 6a). Deposition potential is the electrode potential at which the deposition of the electrolysis product on the electrode surface begins.

The number of electrons involved in the electrode process was also determined from the half-width of the non-stationary voltammetric dependences. For different CrO_3 concentrations, and for scan rates within 0.05-0.2 V/s range, n = 5.7-6.2. For MoO_3 concentrations up to 4 mol %, n = 5.7-6.0, and for concentrations above 4 mol % - 1.7-2.0. In the case of WO_3, for different concentrations, n = 5.7-6.1.

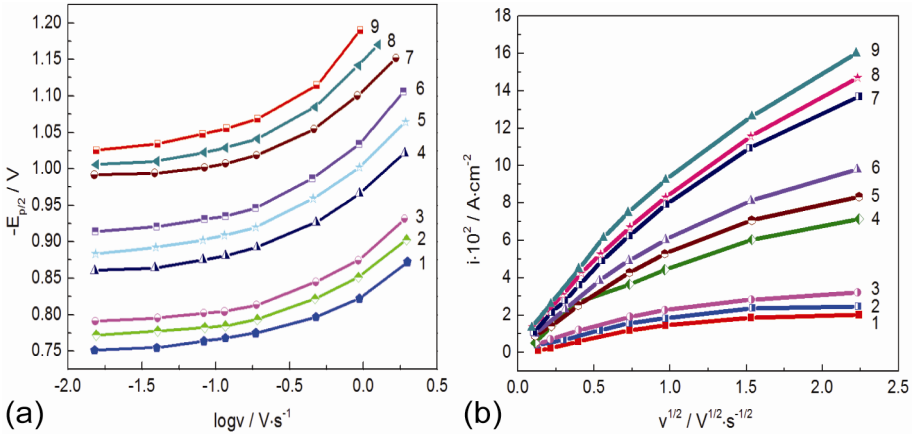

Figure 6. a) Dependence of the half-wave potential on the scan rate at $[MO_3]\times10^4$, mol/cm^3: (1,4,7) -14.0; (2,5,8) - 12.0; (3,6,9) - 10.0; (1-3) - CrO_3 additive; (4-6) - MoO_3; (7-9) - WO_3;
b) Dependence of the peak current on the scan rate at $[MO_3]\times10^4$, mol/cm^3: (1-3) - 6.0; (4-6) - 8.0; (7-9) - 12.0; (1, 4, 7) - MoO_3 addition; (2, 5, 8) - WO_3 addition; (3, 6, 9) - CrO_3 addition.

4. Electrochemical behavior of group VI-B metals in tungstate melts. The group VI-B metals were chosen as electrode materials for the study of multi-electron equilibria and processes. During the study of electroreduction of oxide forms of chromium (molybdenum, tungsten) (VI) on the background of

a tungstate melt, the possibility of the following electrode reactions occurrence was revealed: (4) metal deposition; (5) metal (IV) oxide deposition; (6) metal (III) oxide deposition. To confirm the occurrence of reactions (4) - (6), the electrochemical behavior of chromium (molybdenum, tungsten) electrodes under equilibrium and stationary conditions at a low (2-10 mV/s) scan rate at the same material electrode was studied.

The main method of investigation under equilibrium conditions was potentiometry. For this purpose, we chose the following electrochemical circuits:

$$Cr \mid (1 - x)\ Na_2WO_4 - xCrO_3 \,||\, Na_2WO_4 - 0.2WO_3 \mid O_2 \mid Pt, \quad (7)$$

$$Mo \mid (1 - x)\ Na_2WO_4 - xMoO_3 \,||\, Na_2WO_4 - 0.2WO_3 \mid O_2 \mid Pt, \quad (8)$$

$$W \mid (1 - x)\ Na_2WO_4 - xWO_3 \,||\, Na_2WO_4 - 0.2WO_3 \mid O_2 \mid Pt. \quad (9)$$

The EMFs of circuits (7)-(9) were measured in the range of MO_3 concentrations 0.5÷15 mol % (Fig. 7). The indicator electrodes were chromium (molybdenum, tungsten) polycrystalline rods of the “reagent” grade suspended on a platinum wire. The measurement procedure was similar to that for platinum-oxygen electrodes

Corrosion studies of chromium (molybdenum, tungsten) have revealed corrosion of metals in melts containing small additives of MO_3. This may be why it is not possible to obtain reproducible EMF measuring results at $x < 0.5$ mol % MO_3. The expressions for the potentials of metal and oxide electrodes in accordance with (4)-(6) can be written as follows:

$$E = E^0 + \frac{2.3RT}{6F} \lg \frac{[M_2O_7^{2-}]^4}{[M][MO_4^{2-}]^7} \quad (10)$$

in the case of melt-metal equilibrium;

$$E = E^0 + \frac{2.3RT}{2F} \lg \frac{[M_2O_7^{2-}]^2}{[MO_2][MO_4^{2-}]^3} \quad (11)$$

in the case of melt equilibrium with MO_2 oxide;

$$E = E^0 + \frac{2.3RT}{6F} \lg \frac{[M_2O_7^{2-}]^5}{[M_2O_3][MO_4^{2-}]^8} \quad (12)$$

in the case of equilibrium of the melt with oxide M_2O_3. The calculation of the number of electrons per one electrochemically active particle, calculated from the pre-logarithmic dependence coefficient $dE/d\lg[MO_3]$ (Fig. 7), showed compliance with the six-electron equilibrium for the MoO_3 concentration

range 1÷4 mol %, and for CrO_3 and WO_3 – 1÷15 mol %. The values of E for the corresponding current density values are taken from the experimental dependences in Fig. 8. The two-electron equilibrium corresponds to the MoO_3 concentration range 4÷15 mol %. Electrode reactions (4), (5), and (6) correspond to these values of "n". Melts Na_2WO_4 - (1÷15) mol % CrO_3 are in equilibrium with chromium (III) oxide. Melts Na_2WO_4 - (1÷4 mol %) MoO_3 are in equilibrium with metallic molybdenum, and Na_2WO_4 – (4÷15 mol %) MoO_3 – with MoO_2 oxide. Metallic tungsten is in equilibrium with melts Na_2WO_4 - (1÷15) mol % WO_3.

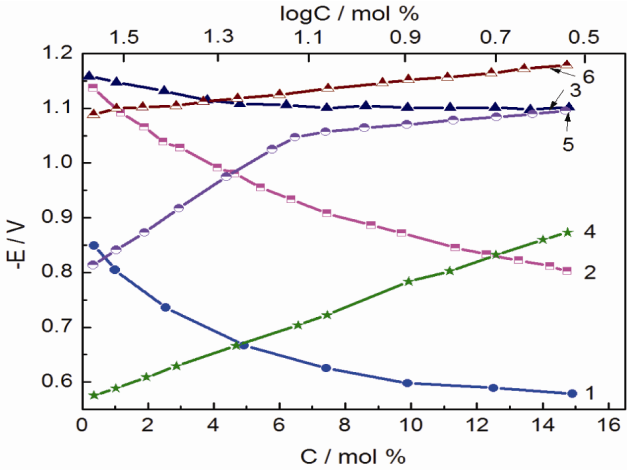

Figure 7. Dependences of the equilibrium potentials of chromium (1, 4), molybdenum (2, 5), and tungsten (3, 6) electrodes on the concentration of the respective oxides in ordinary (1-3) and logarithmic (4-6) coordinates.

The concentration dependences of the equilibrium potentials (4)-(6) are well described by the Nernst equations.

To clarify the nature of the charge transfer stages (4)-(6) for these conditions and to determine the number of electrons transferred in the electrode process, the stationary voltammetric dependences were analyzed in the semilogarithmic coordinate system E–lg(i_d-i). The pre-logarithmic coefficients of the E–lg(i_d-i) dependence for the CrO_3 concentrations 1÷15 mol %, MoO_3 – 1÷4 mol %, and WO_3 – 1÷15 mol. % correspond to reactions involving six electrons (Fig. 8). For the MoO_3 concentrations 4÷15 mol %, the pre-logarithmic coefficient corresponds to the reaction involving two electrons. The good agreement of the coefficients determined from the experimental data with the theoretical ones indicates the reversible nature of the charge transfer stages (4)-(6).

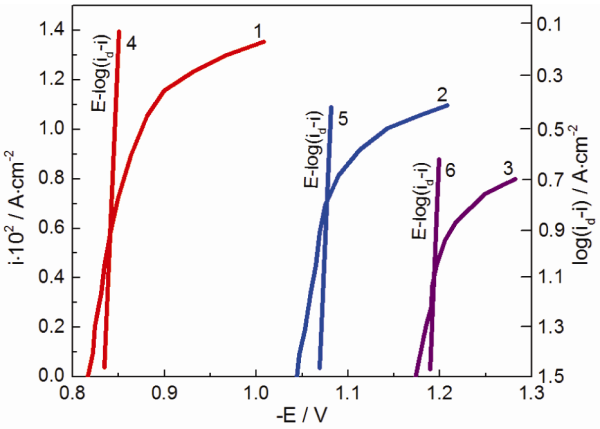

Figure 8. Steady-state voltammetric dependences (1-3) and their analysis in the semilogarithmic coordinate system (4-6). Scan rate = 2 mV/s, T = 1173 K; 1,4 – Cr cathode, [CrO_3] = 3.5 mol %; 2,5 – Mo cathode, [MoO_3] = 2.5 mol %; 3,6 – W cathode, [WO_3] = 2.0 mol %.

Galvano- and potentiostatic electrolysis at CrO_3 concentrations 1÷15 mol % reveals Cr_2O_3, at concentrations of 1÷4 mol % MoO_3 – molybdenum, and at higher concentrations of MoO_3 – molybdenum dioxide. Tungsten is the only product of the electrolysis of systems Na_2WO_4 - (1÷15) mol % WO_3.

CONCLUSIONS

1.The analysis of the present experimental data allows to conclude that multi-electron reversible equilibria involving oxide forms of chromium, molybdenum, and tungsten (VI) can be realized in a sodium tungstate melt.

2.The mechanism and the final product of the electroreduction of metal (VI) oxide forms depend on the acid-base properties of the medium. By setting the latter, the electrode process can be controlled.

3.Of particular note is the uniqueness of the electrode equilibrium involving six electrons at a certain melt basicity.

EXPERIMENTAL SECTION

The study of electrochemical behavior of VI-B group metal oxides in the tungstate melt includes thermodynamic substantiation of the interaction of VI-B group metal oxides with this melt and study of acid-base properties of the tungstate melt by potentiometric method.

The probability of possible interactions between VI-B group metal oxides and sodium tungstate was estimated over a wide temperature range based on the calculations of the change in the standard Gibbs energy (ΔG_T). To calculate ΔG_T, the literature values of the thermodynamic values of the compounds under consideration were used [24, 25].

For potentiometric studies, the melt Na_2WO_4-0.2 mol % WO_3 was chosen as the electrolyte for platinum-oxygen (Pt/O_2) reference electrode in the tungstate melts. The excess of oxygen ion acceptor in it contributes to the oxygen electrode potential stability, which is necessary for the reference electrode functioning. The design of Pt/O_2 reference electrodes of similar composition with a β-Al_2O_3 membrane, the rationale for their use, as well as the method for measuring the equilibrium potentials of Pt/O_2 electrodes, were described in [26, 27].

Na_2WO_4 was selected as the background melt for studying the electrochemical behavior of oxide forms of Group VI B metals. To prepare it, sodium tungstate of the “Reagent” brand was dried at a temperature of 423-473 K for 10-12 hours. It was then calcined at a temperature of 773-873 K for 3-4 hours. The quality of the background melt was determined by measuring the residual voltammetric currents. Their low value at a potential significantly more negative than that of the platinum-oxygen electrode (6 mA/cm^2 at -1.6 V) indicated sufficient purity and suitability for electrochemical measurements. The purity of the background melt was also checked using emission IR spectra. The absence of characteristic bands in the spectrum of the solidified melt meant the absence of impurities.

Metal oxides (VI) of group VI B of the “Reagent” brands were pre-dried at a temperature of 423-473 K for 5-6 hours, and then calcined at 673-773 K for 2-3 hours.

Equilibrium electrode potentials were measured using a SHCH-68003 digital voltmeter. The established value was taken as the one that did not change by $\pm$0.05 unit within 1 hour. Steady-state and transient volt-ampere dependencies were obtained using a PI-50.1 pulse potentiostat. Stationary dependencies were recorded with a two-coordinate recorder PDP-4, and non-stationary ones with an oscilloscope OWON SDS-1022.

A high-temperature cell made of quartz was used to perform electrochemical measurements. A platinum-oxygen electrode was used as a reference electrode, which was a platinum wire with a diameter of 1 mm, half-immersed in a melt of Na_2WO_4 – 20 mol. WO_3. The electrolyte of the reference electrode was separated from the electrolyte under study by an alundum tube with a diameter of 6-8 mm, which acted as a diaphragm. The wall thickness of the tube was 0.5-1 mm. The open end of the tube was connected to the atmosphere. Measurements were carried out in an air atmosphere ($p(O_2)$ 21.3 kPa.

The electrodes used in electrochemical measurements were platinum, chromium, molybdenum, and tungsten wires with a diameter of 0.5-1 mm immersed in the melt. Platinum crucibles served as containers for the melt.

Automatic temperature control with a KVP-1 electronic potentiometer made it possible to maintain the melt temperature with an accuracy of + 2.5 K.

The electrochemical behavior of group VI-B metal oxides in tungstate melt was studied in the range of scan rates 0.02-5.00 V/s using platinum electrodes at a temperature 1173 K, and using electrodes made of group VI-B metals at a scan rate 2 mV/s and a temperature 1173 K.

Diagnostics and estimation of the kinetic parameters of the electrode process were performed based on the theory of stationary and nonstationary electrode processes.

REFERENCES

1. O. Medvezhynska; A. Omelchuk; *Ukr. Chem. J.,* **2023**, *89*(11), 3-34. https://doi.org/10.33609/2708-129X.89.11.2023.3-34
2. M. Erdogan; I. Karakaya; *Metall. Mater. Trans. B,* **2010**, *41*, 798-804. https://doi.org/10.1007/s11663-010-9374-4
3. D. Tang; W. Xiao; H. Yin; L. Tian; D. Wang; *J. Electrochem. Soc.,* **2012**, *159*, E139. https://doi.org/10.1149/2.113206jes
4. V. Malyshev; A. Gab; A.M. Popescu; V. Constantin; *Chem. Res. Chin. Univ.,* **2013**, *29*, 771-775. https://doi.org/10.1007/s40242-013-3003-0
5. V. Malyshev; **2011**, *Mater. Sci., 47*(3), 345-354. https://doi.org/10.1007/s11003-011-9402-9
6. N.B. Sun; Y.C. Zhang; F. Jiang; S.T. Lang; M. Xia; *Fusion Eng. Des.,* **2014**, *89*(11) 2529-2533. https://doi.org/10.1016/j.fusengdes.2014.05.027
7. V. Malyshev; A. Gab; D. Shakhnin; C. Donath; E.I. Neacsu; A.M. Popescu; V. Constantin; *Rev. Chim.,* **2018**, *69*(9), 2411-2415. https://doi.org/10.37358/RC.18.9.6544
8. A. Gab; V. Malyshev; D. Shakhnin; A.M. Popescu; V. Constantin; *Studia UBB Chemia,* **2024**, *69*(1), 35-50. https://doi.org/10.24193/subbchem.2024.1.03
9. Y.H. Liu; Y.C. Zhang; Q.Z. Liu, X.L. Li; F. Jiang; *Fusion Eng. Des.,* **2012**, *87*(11), 1861-1865. https://doi.org/10.1016/j.fusengdes.2012.09.003
10. V. Malyshev; A. Gab; A.M. Popescu; V. Constantin; *Rev. Chim.,* **2011**, *62*(11), 1128-1130. https://doi.org/10.37358/Rev.Chim.1949
11. V. Malyshev; A. Gab; A. Survila; C. Donath; E.I. Neacsu; A.M. Popescu; V. Constantin; *Rev. Chim.,* **2019**, *70*(3), 871-874. https://doi.org/10.37358/RC.19.3.7023
12. M. Mann; S.E. Shter; G.M. Reisner; G.S. Gideon; *J. Mater. Sci.,* **2007**, *42*, 1010-1018. https://doi.org/10.1007/s10853-006-1384-x
13. V. Malyshev; H. Kushkhov; V. Shapoval; *J. Appl. Electrochem.,* **2002**, *32*, 573-579. https://doi.org/10.1023/A:1016544524468

14. V. Malyshev; A. Gab; D. Shakhnin; A.M. Popescu; V. Constantin; *Rev. Roum. Chim.,* **2010**, *55*(4), 233-238.
15. V. Malyshev; D. Shakhnin; A. Gab; I. Astrelin; L. Molotovska; V. Soare; C. Donath; E.I. Neacsu; V. Constantin; A.M. Popescu; *Rev. Chim.,* **2016**, *67*(12), 2490-2500. https://doi.org/10.37358/Rev.Chim.1949
16. V. Malyshev; A. Gab; D. Shakhnin; C. Donath; E.I. Neacsu; A.M. Popescu; V. Constantin; *Rev. Chim.,* **2018**, *69*(9), 2411-2415. https://doi.org/10.37358/RC.18.9.6544
17. V.L. Cherginets; *Electrochim. Acta,* **1997**, *42*(10), 1507-1514. https://doi.org/10.1016/S0013-4686(96)00308-8
18. V.L. Cherginets; Oxoacidity: *Reactions of Oxo-compounds in Ionic Solvents*. Elsevier Science, **2005**. ISBN: 978-0-444-51782-1
19. V.A. Onischenko; V.V. Soloviev; L.A. Chernenko; V.V. Malyshev; S.N. Bondus; *Materialwisse. Werkst.,* **2014**, *45*(11), 1030-1038. https://doi.org/10.1002/mawe.201400222
20. V.V. Malyshev; V.V. Soloviev; L.A. Chernenko; V.N. Rozhko; *Materialwiss. Werkst.,* **2015**, *46*(1), 5-9. https://doi.org/10.1002/mawe.201400331
21. NIST-JANAF, in: J.M.W. Chase; Ed., *Thermochemical Tables*
22. fourth ed., Proceedings of the American Chemical Society and the
23. American Institute of Physics, New York, NY, **1999**.
24. C.E. Lucke; *Handbook of Thermodynamic Tables and Diagrams*. Forgotten Books. **2020**. ISBN: 978-0484660105
25. G. Inzelt; A. Lewenstam; F. Scholz; Eds., *Handbook of Reference Electrodes*. Heidelberg: Springer Berlin. **2013**. ISBN: 978-3-642-44873-7
26. *NIST-JANAF Thermochemical Tables*. Malcolm W. Chase Jr., Ed. *Anal. Chem*., **1999**, *71*(5), 218A. 1952 p. https://doi.org/10.1021/ac991732g
27. C.E. Lucke; *Handbook of Thermodynamic Tables and Diagrams*. Forgotten Books, **2018**. 256 p. ISBN: 978-0484660105
28. S. Somia; *Handbook of Advanced Ceramics. Materials, Applications, Processing, and Properties*. Academic Press, **2013**. ISBN: 978-0-12-385469-8
29. S.Y. Kwon; R.J. Hill; I.H. Jung; *A model for multicomponent diffusion in oxide melts*. *CALPHAD 72*, 102246, **2021**. https://doi.org/10.1016/j.calphad.2020.102246